Appl. Phys. B 68, 257–265 (1999)

Applied Physics B
Lasers
and Optics

Multiplex CARS measurements in supersonic H_2/air combustion

S.-R. Yang[1,*], **J.-R. Zhao**[1], **C.-J. Sung**[2], **G. Yu**[1]

[1] Chinese Academy of Sciences, Beijing 100080, P.R. China
[2] Princeton University, Princeton, NJ 08544, USA

Received: 1 July 1997/Revised version: 29 September 1998

Abstract. H_2 and O_2 multiplex coherent anti-stokes Raman spectroscopy (CARS) employing a single dye laser has been explored to simultaneously determine the temperature and concentrations of H_2 and O_2 in a hydrogen-fueled supersonic combustor. Systematic calibrations were performed through a well-characterized H_2/air premixed flat-flame burner. In particular, temperature measurement was accomplished using the intensity ratio of the H_2 S(5) and S(6) rotational lines, whereas extraction of the H_2 and O_2 concentrations was obtained from the H_2 S(6) and O_2 Q-branch, respectively. Details of the calibration procedure and data reduction are discussed. Quantification of the supersonic mixing and combustion characteristics applying the present technique has been demonstrated to be feasible. The associated detection limits as well as possible improvements are also identified.

PACS: 33.20; 42.65

In response to the interest in the development of scramjet engines and the fundamental understanding of supersonic combustion and mixing processes, extensive experimental research has been performed to quantitatively measure the desirable parameters characterizing the various physical phenomena under supersonic combustion. Of particular interests are the concentrations of fuel, oxidizer, and combustion major/minor products as well as the temperature distribution. Laser diagnostics of high spatial and temporal resolutions offer excellent tools to meet such needs.

Among the various laser-based techniques, coherent anti-Stokes Raman spectroscopy (CARS) has been recently demonstrated to be an attractive approach for the determination of the temperature and major species in supersonic combustors [1–3]. In addition, in order to maximize data collection and develop parameter correlations within the short duration of facility operation, recent developments in multicolor CARS techniques make simultaneous measurements of multiple species available [1, 2]. As such, information describing mixing and combustion rates in supersonic flows can be effectively extracted. However, multi-color CARS technique requires multiple dye lasers for the Stokes incidences and more complicated optical arrangement. Moreover, such a technique has to account for the interactions between signals resulting from all of the excited Raman transitions owing to the complex, nonlinear CARS process. Inevitably, this may involve assumptions of a variety of unknowns in data analysis [2].

Since hydrogen is one of the preferred fuels for scramjet engines and its vibrational/rotational transitions are relatively widely spaced, attempts of multiplex CARS have been made for the simultaneous measurement of temperature and species using a single dye laser as long as the Raman frequencies of these species differ by less than the linewidth of the dye laser for the Stokes beam. In particular, our previous study [4] has demonstrated that multiplex CARS measurements of H_2 and O_2 seem to be feasible in supersonic combustors. Particularly, the O_2 Q-branched bandhead (Raman shift 1556 cm^{-1}) is sandwiched by the H_2 pure rotational lines of S(5) (Raman shift 1447 cm^{-1}) and S(6) (Raman shift 1637 cm^{-1}) when the temperature is beyond 700 K. Therefore, extraction of information regarding temperature and local equivalence ratio are possible within a single measurement. This approach is especially significant when nitrogen is not a constituent of the oxidizer such that N_2 CARS cannot be utilized for combustion thermometry, for instance in LOX/LH_2 rocket engine.

The present study aims to extend our previous effort [4] in the following two-step manner, with emphasis on the application to the diagnostics of supersonic reacting flows. Namely, (i) calibrations of temperature and species concentrations through a well-characterized flat-flame configuration; (ii) quantification of temperature and the extent of mixing in a supersonic combustor.

In terms of the former, we first note that while [4] has demonstrated the potential usefulness of the proposed multiplex CARS, the actual procedures for quantification have not yet been rationalized. In addition, since the line-broadening processes of H_2 CARS is not well established as compared to that of N_2 CARS, theoretical spectra of H_2 CARS become

* Corresponding author. Dept. of Laser Technology, Institute of Mechanics, Chinese Academy of Sciences, 15 Zhong Guan Cun Road, Beijing, 100080, P.R. China; Fax: +86-10/6256-1284; E-mail: yangsr@cc5.imech.ac.cn

questionable. It is therefore of importance to conduct a series of experiments to calibrate the correlation between the intensity ratio of H_2 lines of S(5) and S(6) and temperature.

In order for the calibration to be meaningful, it is essential that the flame configuration is well defined for both experimental and computational quantification. One such configuration is the burner-stabilized flat-flame which offers a simple, well-controlled environment through which the flame structure can be studied with reasonable confidence. Here, a steady, planar flame is stabilized through heat loss to the porous surface of a flat burner, from which the combustible mixture is introduced. Due to its simplicity in experimentation and the nature of one-dimensionality, we shall use the burner-stabilized flat-flame burner as a calibration tool for both temperature and species concentrations over a wide range of mixture stoichiometries. Through detailed comparisons of the N_2 CARS and H_2 CARS in this well-characterized flame, the temperature dependence of the intensity ratio of S(5) and S(6) can be calibrated. Subsequently, approaches in obtaining the concentrations of H_2 and O_2 are systematically studied.

After accomplishing the above-mentioned calibration procedures, the second objective of the present study is to explore the feasibility of the experimental identification of the mixing and combustion characteristics in a supersonic hydrogen/air mixture, applying multiplex CARS. Through simultaneous determination of the temperature and local equivalence ratio, it greatly enhances the understanding of supersonic mixing and combustion processes as well as provides insight into the numerical simulation in practical supersonic combustors.

In the next section we shall sequentially present the experimental details, including the theoretical background of CARS, the present optical arrangement of CARS, the flat-flame burner, and the supersonic combustion facility. This is followed by presentation of the calibration procedure and results, and then discussion of the measurements in supersonic combustion.

1 Experimental details

1.1 CARS overview

CARS is a nonlinear four-wave mixing process. When two pump beams at frequency ω_p and one Stokes beam (dye beam) at frequency ω_s are phase-matched and focused in a medium, a laser-like coherent beam at frequency $\omega_{as}(\omega_{as} = 2\omega_p - \omega_s)$ called the CARS signal is generated. When the frequency difference $(\omega_p - \omega_s)$ is close to a Raman resonance in a particular species, the CARS signal is resonantly enhanced. This is known as resonant CARS. The intensity of a CARS signal is proportional to the square of the third-order nonlinear susceptibility of the medium, $\chi^{(3)}$,

$$I_{as}(\omega_{as}) \propto I_p^2(\omega_p) I_s(\omega_s) |\chi^{(3)}|^2 , \tag{1}$$

where I_p and I_s are the intensities of the pump and Stokes lasers, respectively. The third-order nonlinear susceptibility of the medium is expressed as

$$\chi^{(3)} = \frac{N}{\hbar} \sum_j \frac{\alpha_j^2 \Delta\rho_j}{(\omega_j - \omega_p + \omega_s) - \mathrm{i}\Gamma_j} + \chi_{NR} , \tag{2}$$

where N is the number density of the probed species, ω_j the Raman transition frequency, Γ_j the Raman linewidth, α_j the polarizability matrix element, $\Delta\rho_j$ the population difference between the upper and lower states of the rotational-vibrational transitions with frequency ω_j which is a function of temperature, and χ_{NR} the dispersionless real nonresonant susceptibility.

For a pure rotational S-branch transition, the susceptibility can be expressed as

$$\chi^{(3)} = \frac{N}{\hbar} \frac{\Delta\rho_j}{(\omega_j - \omega_p + \omega_s) - \mathrm{i}\Gamma_j} \frac{4}{45} \gamma^2 b_{J+2}^J K(J) + \chi_{NR} , \tag{3}$$

where γ is the anisotropic polarizability, b_{J+2}^J the Placzek–Teller coefficients, $K(J)$ the first-order line strength correction factor for the centrifugal distortion,

$$K(J) = \left[1 \frac{4}{\eta} \left(\frac{B_e}{\omega_e} \right)^2 (J^2 + 3J + 3) \right]^2 , \tag{4}$$

$\eta = \gamma(r_e \partial\gamma/\partial r|_{r_e})^{-1}$, B_e the rotational constant, ω_e the molecular vibrational frequency, and r_e the internuclear distance.

While measurement of temperature can be performed from the shape of the spectral signature of N_2 [5], the intensity ratio of two pure rotational states of H_2 is temperature dependent [6], and hence can be readily applied to yield the temperature information. Furthermore, species measurement can be obtained from the intensity of the spectrally integrated resonant CARS signal [5]. However, this approach is plagued by the presence of the background at very low concentrations in that the modulation would disappear into a baseline level derived from the nonresonant susceptibility [5]. Such a difficulty can be circumvented with background suppression, while the signal loss of resonant-mode accompanies the suppression of the nonresonant contributions.

1.2 CARS facility

USED CARS (unstable-resonator spatially enhanced detection) [5], a two-beam 3-D phase-matching configuration, is utilized for its ease of alignment, simple access requirement, and insensitivity to refractive index variations. The associated experimental scheme is shown in Fig. 1. A Nd:YAG (Spectra-Physics, GCR 290-30) laser with a pulse repetition rate of 30 Hz outputs a Gaussian beam at 1.06 μm. After frequency doubling, the green beam at 532 nm is split into two beams by the beam splitter, BS. The reflected beam (about 50 mJ/pulse) is used as the pump beam, and the transmitted portion (about 300 mJ/pulse) is used to pump a broadband dye laser (Spectrum Master, HD-500B). A dye-methanol mixture of 1×10^{-4} mole (53 mg/l) Rhodamine 590 and 1.5×10^{-5} mole (8 mg/l) Rhodamine 610 is used to produce a Stokes beam of ≈ 30 mJ/pulse with a center wavelength of 580.4 nm and a bandwidth of 120 cm^{-1} FWHM, for H_2 and O_2 multiplex CARS. For N_2 CARS, a methanol solution of 2×10^{-4} mole (118 mg/l) Rhodamine 640 is used to produce a Stokes radiation of ≈ 20 mJ/pulse with a center wavelength of 606.7 nm and a FWHM of 100 cm^{-1}.

An annular mirror, AM, with a drilled 45 degree angle aperture of 4 mm diameter passes the Stokes beam through the center and reflects the pump beam, as shown in Fig. 2. It

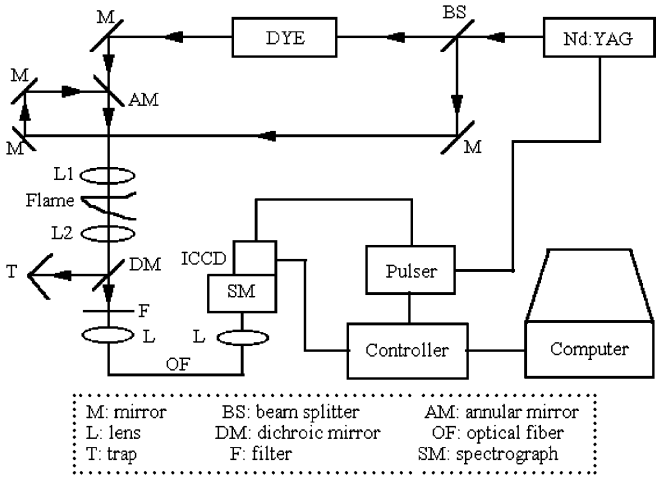

Fig. 1. Schematic diagram for the USED CARS setup

renders the Gaussian annular pump beam in a USED CARS phase-matching configuration. The use of such an annular mirror provides better transmission of ω_s than a dichroic mirror does as well as the flexibility for different Stokes beams required by various probed species.

Using a 200-mm focal length lens, L_1, the annular pump and Stokes beams are focused on the measuring point where the CARS signal is generated. The pump and Stokes beams and CARS signal along with the laser beams in the forward direction are recollimated using a second 200-mm lens, L_2. The resulting spatial resolution is ≈ 4 mm along the beam and $\approx 100\,\mu$m transverse to the beam. A dichroic mirror, DM, reflects the high intensity pump and Stokes beams, and transmits the CARS signal. The pump and Stokes beams are trapped by a dump, T. The transmitted portion of the pump and Stokes beams are spectrally filtered from the CARS signal by an interference filter, F. The CARS signal transmitted through an optical fiber, OF, is focused on a slit of SPEX-500M monochromator, SM. A holographic grating of 2400 lines/mm is utilized to disperse the CARS signal, and then a CARS spectrum images on an intensified CCD, (PI, ICCD 1152MG-E). The CARS spectra are then collected, recorded, and analyzed.

It is also noted that the dye-laser profile is monitored during experimentation, which can thus be used to normalize the CARS spectra.

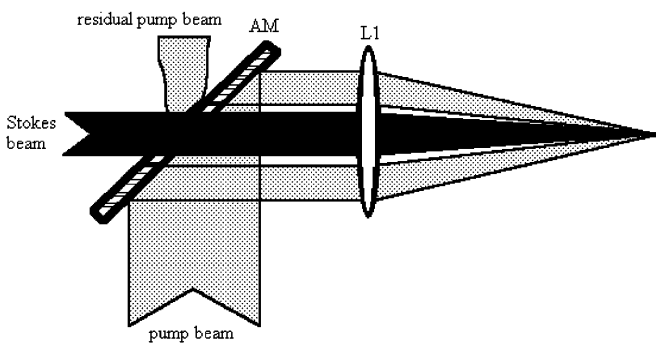

Fig. 2. Laser beam arrangement for the phase-matching geometry of USED CARS

1.3 Flat-flame burner

The burner used for the present calibration experiments is made of porous sintered bronze with a 20 μm pore size and 50 mm diameter. A sectional view of the burner is shown in Fig. 3. The body of the flat-flame burner is made of brass, with an outer diameter of 100 mm and a height of 50 mm. Cooling is accomplished by passing water at a controlled rate through cooling coils imbedded in the burner. A circular porous ring is placed around the main burner to provide a uniform coflow of the inert gas to shield the flame from the environment. The flows of fuel and air are controlled by sonic nozzle flowmeters. The flowmeters have been calibrated with a wet test meter. The flows of fuel and dry air are mixed in a premixing reservoir.

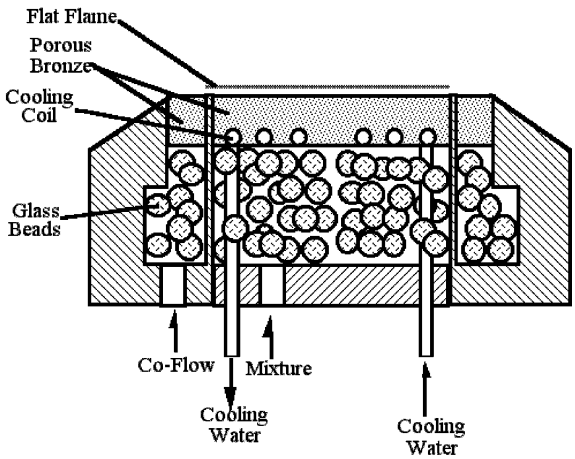

Fig. 3. Sectional view of the flat-flame burner

1.4 Supersonic combustor

The test facility used has been discussed in detail elsewhere [7, 8]. The vitiated air of temperature 2100 K and pressure 2.0 MPa can be produced by a heater burning hydrogen/air along with oxygen replenishment. The flow rate can be as high as 1.5 kg/s.

The combustor is of rectangular cross section with an inlet dimension of 30 mm × 30 mm and overall length of 755 mm. The hydrogen injector and the air nozzle are designed in an integrated modular structure. Hydrogen is injected by a strut base through a double row of multiple orifices of 1.8 mm diameter. The two rows of orifices have angles of 30° and 45°, respectively. The blade-like strut is mounted in the center of the combustor entrance. The upper and lower contour walls of the strut and the combustor wall form two half-parts of a nozzle, which produces a two-dimensional supersonic air flow of Mach number 2.5. Hydrogen is injected into the supersonic vitiated air with sonic speed.

A sectional view of the supersonic combustor test section is shown in Fig. 4, where three holes with a diameter of 8 mm are available for the access of the probe laser beams. A typical experiment running time is 7 s. The supersonic flow field has been shown to reach steady state within 2 s [7]. CARS measurement is conducted after hydrogen is injected and supersonic combustion is sustained.

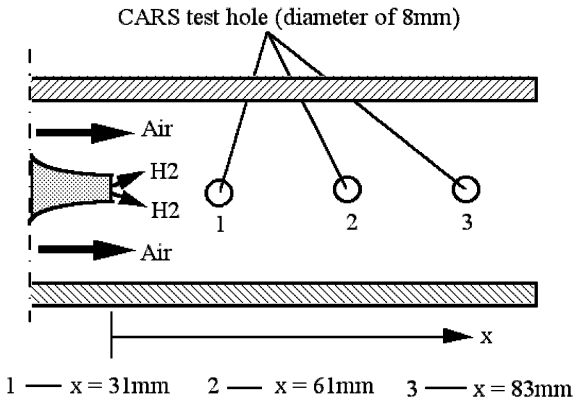

Fig. 4. Sectional view of the test section of the supersonic combustor

2 Calibration details

2.1 Computational specifications

2.1.1 Spectroscopy calculations. Libraries of theoretical CARS spectra, including those of N_2, H_2, and O_2, are computed using the CARSFT [9] code developed at Sandia National Laboratories. Subsequent comparisons with the experimental spectra would provide insights to temperature and species concentrations.

The slit instrument function employed to generate the theoretical CARS spectra is obtained by using a He-Ne laser with the experimental optical arrangement.

2.1.2 Flame calculations. Simulation of a one-dimensional burner-stabilization flame structure can be conducted employing the PREMIX code of Kee et al. [10]. The program uses finite differences to solve the governing equations of mass, species, and energy conservation with detailed kinetics and species diffusion. However, in order for a direct, meaningful comparison between computation and measurement, accurate experimentally determined boundary conditions, such as the burner surface temperature, are required as inputs to the PREMIX code. Alternatively, local equilibrium assumption has been shown to be an adequate and expedient approach for the calibration experiments using a flat-flame burner [11]. Figures 5 and 6 plot the computed profiles of temperature and major species for lean and rich H_2/air flames, respectively, where burner surface temperature is kept constant at 330 K. It is seen that both the temperature and mole fractions of major species are nearly invariant beyond 1 mm above the burner surface. In addition, Figs. 5 and 6 demonstrate that local equilibrium calculations based on the local temperature agree very well with the ones obtained from detailed simulations, when the distance above the burner surface is beyond 1 mm. Even the largest error associated with H_2 in rich burning is still around 3%, which is smaller than the typical experimental uncertainty. Local equilibrium calculations are performed with the EQUIL [12] code of Sandia National Laboratories. The reaction mechanism used is taken from Kim et al. [13].

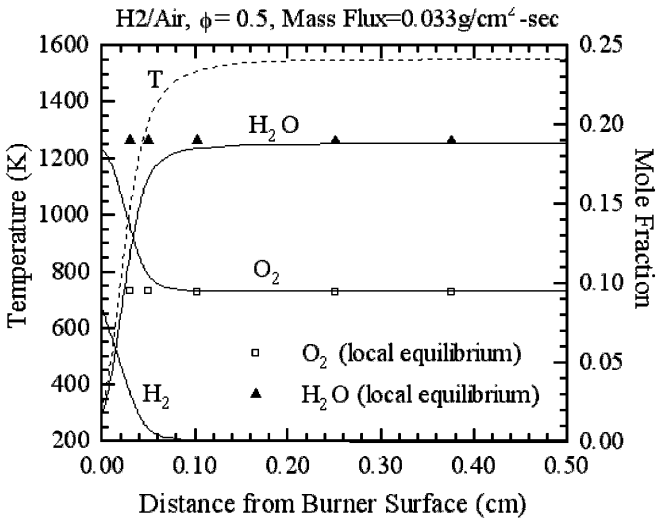

Fig. 5. Comparison of detailed calculation and approximation based on local equilibrium, for a H_2/air flame of equivalence ratio $\phi = 0.50$

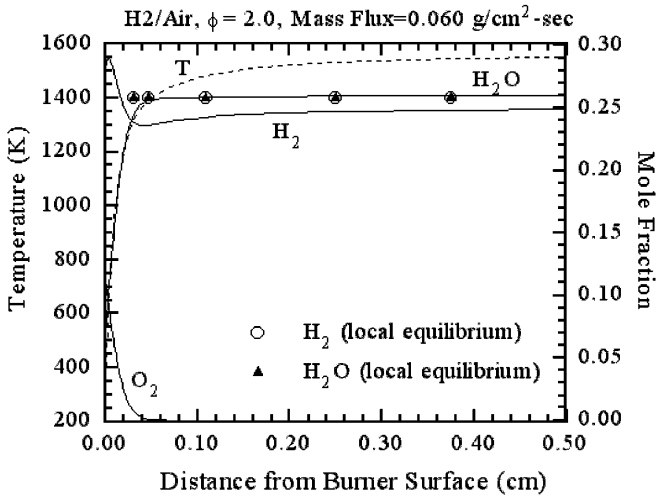

Fig. 6. Comparison of detailed calculation and approximation based on local equilibrium, for a H_2/air flame of equivalence ratio $\phi = 2.0$

2.2 Calibration procedure

Calibration of temperature and the concentrations of H_2 and O_2 is conducted through the H_2/air premixed flat-flame burner, over a wide range of equivalence ratios. For a given flame condition, N_2 CARS spectra and H_2-O_2 multiplex CARS spectra are obtained separately, while being measured at the same position above the burner surface. Due to the extensive regime of uniformity downstream of the flat flame, error resulting from the possible, slight mismatching in the probed position is greatly minimized. Furthermore, since H_2 and O_2 are, respectively, the deficient species in the lean and rich burning conditions, calibration of H_2 (O_2) alone can be unambiguously performed under various rich (lean) stoichiometries.

2.2.1 Calibration of temperature. The measured temperature is first determined from the N_2 CARS spectrum through a nonlinear least-square fitting using CARSFT. Two-parameter fitting, including temperature and nonresonant susceptibility, are utilized because the composition of the burnt product is unknown. This N_2 CARS-determined temperature is

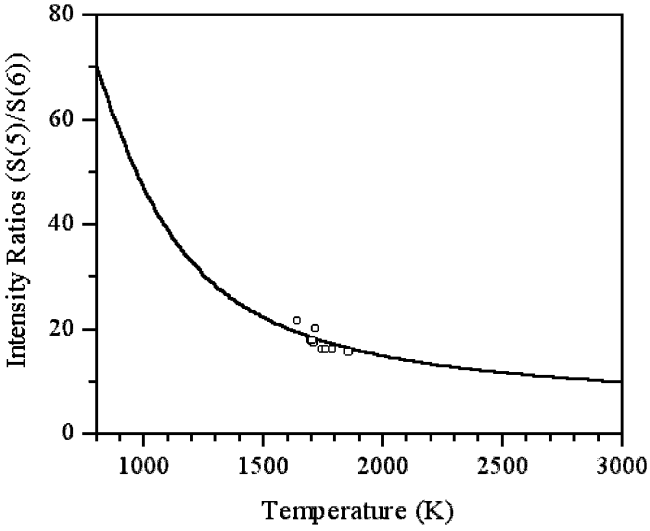

Fig. 7. Calibration of the calculated resonant intensity ratios of the H_2 S(5) and S(6) as a function of temperature. *Symbols* represent the experimental data from the calibration experiments. *Solid line* is the theoretical calculation

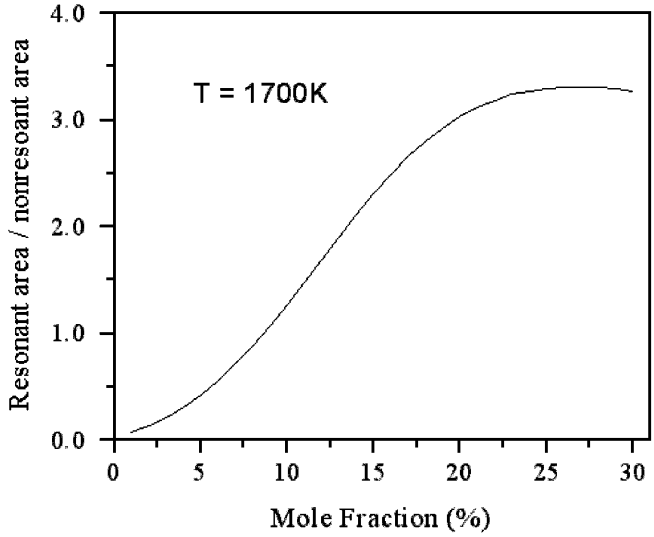

Fig. 9. Computed ratio of the spectrally integrated resonant and nonresonant signals of O_2 (from 1536 cm^{-1} to 1560 cm^{-1}) as a function of O_2 mole fraction at temperature of 1700 K

subsequently used to calibrate the H_2 CARS spectrum at the corresponding experimental condition.

In addition, the theoretical dependence of the resonant intensity ratio of H_2 S(5) and S(6) on temperature is calculated with the soft-collision model [14] incorporating Doppler broadening, which is shown in Fig. 7. The spectra are computed ranging from 1407 cm^{-1} to 1487 cm^{-1} for S(5) and from 1597 cm^{-1} to 1677 cm^{-1} for S(6), respectively.

2.2.2 Calibration of O_2 *mole fraction.* When the local temperature is known, the determination of O_2 mole fraction is based on the fact that concentration is a function of the ratio of the spectrally integrated resonant and nonresonant CARS spectra. Therefore, once the temperature is determined, the O_2 mole fraction is calibrated based on the local equilibrium calculation.

However, one limitation of this ratio method for the species measurement is that only a finite range of the mole fraction is applicable [5]. Taking the temperature of 1700 K as an example, Fig. 8 illustrates the computed normalized O_2 CARS spectra at various mole fractions. Figure 9 further plots the correlation of the ratio of the spectrally integrated resonant and nonresonant signals with variations of the O_2 mole fraction. The integration is taken from 1536 cm^{-1} to 1560 cm^{-1}, with the assumption that the nonresonant intensity varies linearly with the Raman shift. Thus, the resonant area is determined from the total spectral area subtracting the nonresonant area. It is seen from Fig. 9 that the accurate determination of O_2 mole fraction is only applicable from 1% to 25%, at the temperature of 1700 K. The lower bound is due to the hampering of the nonresonant contribution, whereas the upper bound is due to the insensitivity of the signal area ratio to the mole fraction variations.

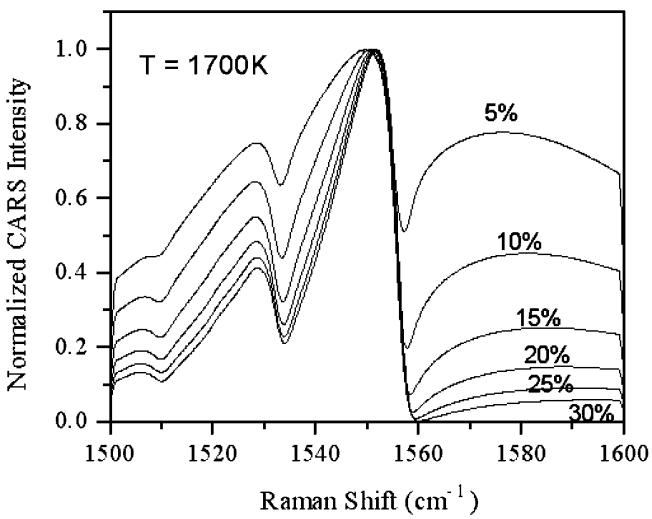

Fig. 8. Computed normalized CARS spectra of O_2 at various mole fractions, with temperature of 1700 K

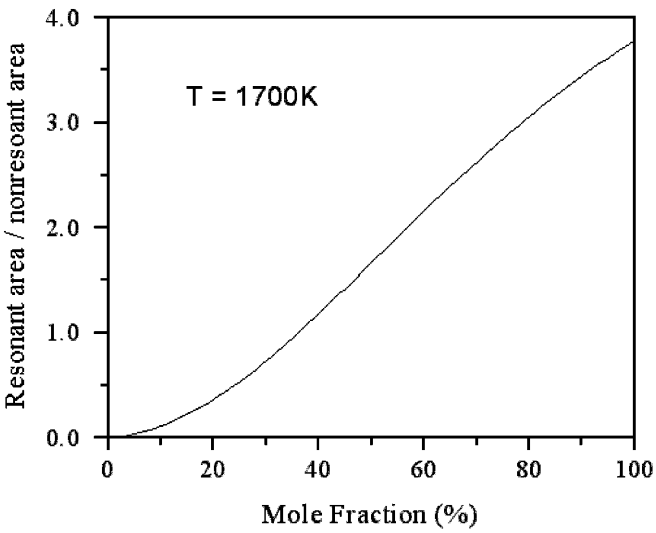

Fig. 10. Computed ratio of the spectrally integrated resonant and nonresonant signals of the H_2 S(6) line (from 1636 cm^{-1} to 1642 cm^{-1}) as a function of mole fraction at temperature of 1700 K

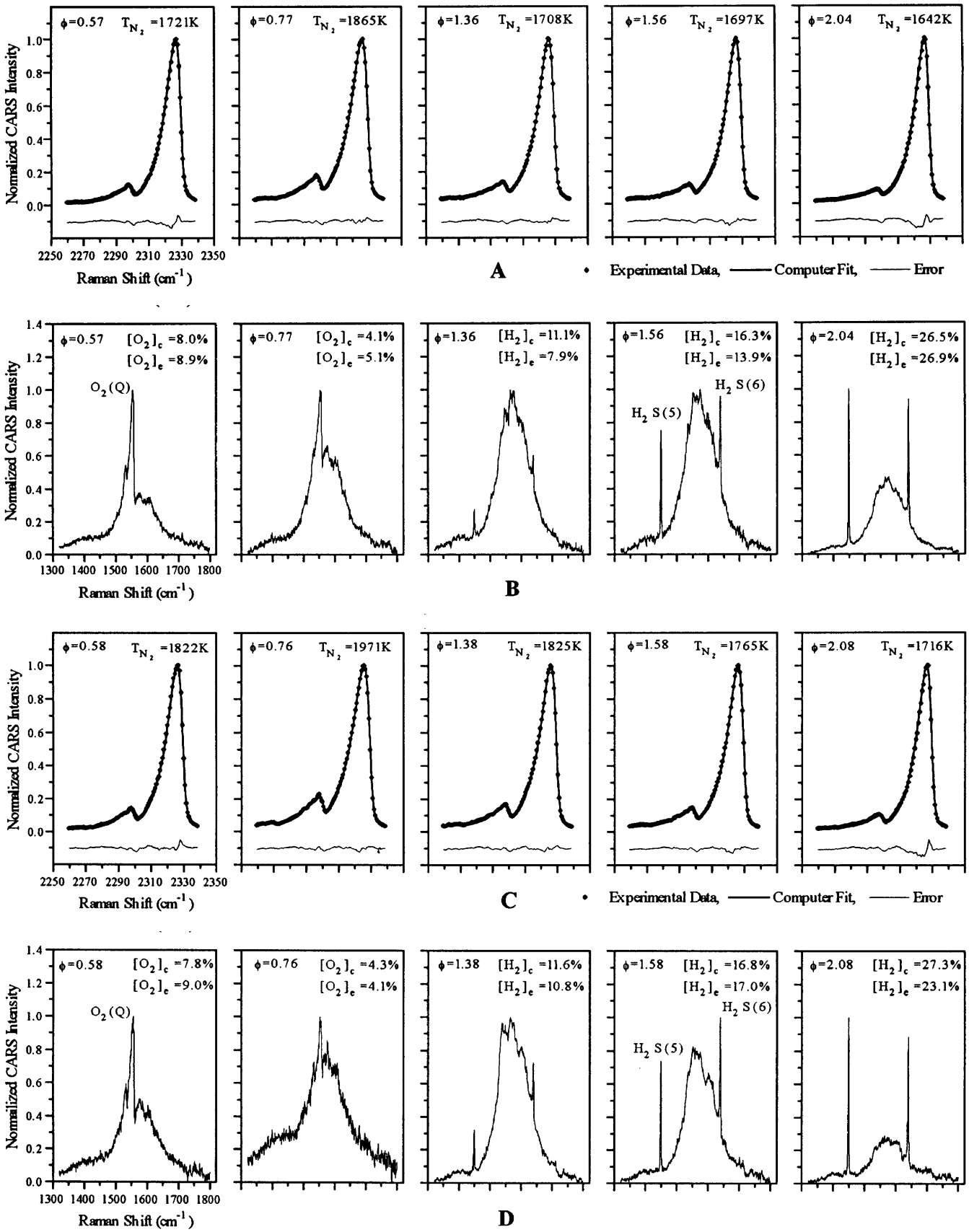

Fig. 11. N_2 (**a**, **c**) and H_2-O_2 CARS spectra (**b**, **d**) taken in the H_2/air premixed flat flames. The measured temperatures and the mole fractions of H_2 and O_2 are denoted in the figures. T_{N_2} is the temperature derived from the N_2 CARS spectrum, $[H_2]_e$ and $[H_2]_c$ the mole fractions of H_2 derived from the H_2 S(6) line and the local equilibrium calculation, $[O_2]_e$ and $[O_2]_c$ the mole fractions of O_2 derived from the O_2 Q-branch and the local equilibrium calculation, respectively. ϕ–equivalence ratio. **a**, **b**–total flow rate of H_2 + air is 44 SLPM; **c**, **d** –85 SLPM

2.2.3 Calibration of H_2 *mole fraction.* The H_2 mole fraction can also be determined from the ratio of the spectrally integrated resonant and nonresonant CARS spectra. Again, calibration is accomplished with the local equilibrium calculation through the flat-flame experiment, at a given measured temperature.

If H_2 Q-branch CARS spectra were used, it is difficult to accurately determine the nonresonant area because the nonresonant signal is much weaker than the resonant one. On the other hand, the S(5) and S(6) lines of H_2 are weak and hence the nonresonant contribution can be easily identified. The computed correlation of the ratio of the spectrally integrated resonant and nonresonant areas for the S(6) line with the mole fraction variations is demonstrated in Fig. 10 at temperature of 1700 K. The integration region is from 1636 cm^{-1} to 1642 cm^{-1}. It is seen that a much wider range of mole fractions is applicable comparing to that of O_2 Q-branch CARS. The lower detection limit is less than 0.05. It is also noted that although the intensity of S(5) is typically nine times that of S(6) at the same pumping condition, the choice of S(6) in experimentation is simply because S(5) is excited by the weaker wing of the Stokes profile such that its nonresonant signal is too small to be determined.

3 Results and discussion

Figure 11 shows the calibration results using the H_2/air premixed flat-flame burner, over a wide range of equivalence ratios. Each experimental spectrum is the average over 1500 laser shots. Figure 11a,b is for the total flow rate of 44 SLPM (standard liter per minute), while the total flow rate of $H_2 +$ air in Fig. 11c,d is kept at 85 SLPM. In general, the flat flame is closer to the corresponding adiabatic condition with increasing flow rate due to the reduced heat loss to the burner.

Again, the N_2 CARS spectra are utilized to determine the corresponding temperatures for the local equilibrium calculations as well as for the calibration of H_2 thermometry. T_{N_2} denotes the temperature derived from the N_2 spectrum. In addition, $[O_2]_e$ and $[H_2]_e$ are the experimentally determined mole fractions of O_2 and H_2, respectively, based on a series of theoretical calculations similar to those in Figs. 9 and 10. Moreover, $[O_2]_c$ and $[H_2]_c$ are, respectively, the computed mole fractions of O_2 and H_2 through the local equilibrium calculation at the temperature of T_{N_2}. Furthermore, the reproducibility of the calibration experiments is within 5%.

3.1 Temperature

Experimentally, in order to achieve an accurate determination of the intensity ratio of S(5) and S(6), three corrections needed to be carefully accounted for. First, the spectral lineshape of the Stokes profile has to be accounted for because it determines the CARS intensity of each Raman shift (see (1)). In the present study, while the frequency of S(5) and S(6) differs by 190 cm^{-1}, the FWHM of the applied Stokes profile is only 120 cm^{-1}. In addition, the center of the Stokes beam lies at 580.4 nm. As a result, the intensity of the Stokes beam exciting S(5) is only 14 percent of that for S(6). Appropriate adjustment of each measured spectrum is thus exercised.

The other two corrections are due to the spectral transmittance of the optics and the spectra responsivity of ICCD. The former mainly resulted from the interference filter and the dichroic mirror used in the optical arrangement. The experimentally determined correction factors of S(5)/S(6) for the optics and ICCD are 0.88 and 0.86, respectively.

The temperature derived from the N_2 CARS spectrum as well as the corresponding experimental and theoretical intensity ratios of H_2 S(5) and S(6) lines are compared in Fig. 7, in which symbols represent the experimental data. It is seen that the discrepancy between T_{N_2} and the H_2 CARS-determined one is within 100 K, for the temperature range studied herein. The average error is approximately four percent.

3.2 O_2 *mole fraction*

Since the lineshape of the nonresonant signal is typically a mirror image of the Stokes profile [15], it can be considered to resemble a Gaussian profile. Therefore, for the integration of the spectral area discussed earlier, the nonresonant spectral area is approximated as a trapezium. Although this integrated nonresonant area could include a portion of the resonant signal, only a small error is expected to be introduced because both the theoretical and the experimental spectra are processed with the same procedure.

Figure 11 shows that the difference between $[O_2]_e$ and $[O_2]_c$ is about 14 percent. Whereas the applicable range of O_2 mole fraction for experimentation is estimated to be from one percent to twenty-five percent based on the theoretical calculation shown in Figs.8 and 9, the actual lower detection limit of O_2 is about four percent. Such an experimental difficulty is caused by the low signal-to-noise ratio when the mole fraction of O_2 is less than 4 percent, especially the hot band disappears into the background. Additional experiments also demonstrate that the resonant signal of O_2 is no longer detectable when the equivalence ratio of H_2/air is greater than 0.8.

3.3 H_2 *mole fraction*

Theoretically, the estimated lower detection limit of the H_2 mole fraction can be less than five percent as shown in Fig. 10. However, Fig. 11 illustrates that the lower experimental detection limit of H_2 is about ten percent. In addition, resonant signal of H_2 CARS is not detectable when the equivalence ratio of H_2/air is less than 1.4. Fig. 11 also shows that the difference between $[O_2]_e$ and $[O_2]_c$ is about 12 percent.

4 Application to supersonic combustion

After accomplishing the above systematic calibrations, we shall explore the feasibility of the proposed multiplex CARS applying to the supersonic H_2-air combustion, with emphasis on the simultaneous determination of the temperature and the mole fractions of H_2 and O_2. Figure 12 demonstrates such a feasibility.

The supersonic condition is established through a stagnation pressure of 1.66 MPa, stagnation temperature of 1500 K, and the global equivalence ratio of 0.5. The resulting static pressure within the test section is around atmospheric (≈ 0.095 MPa). Spectra of Fig. 12 are the averages over 30

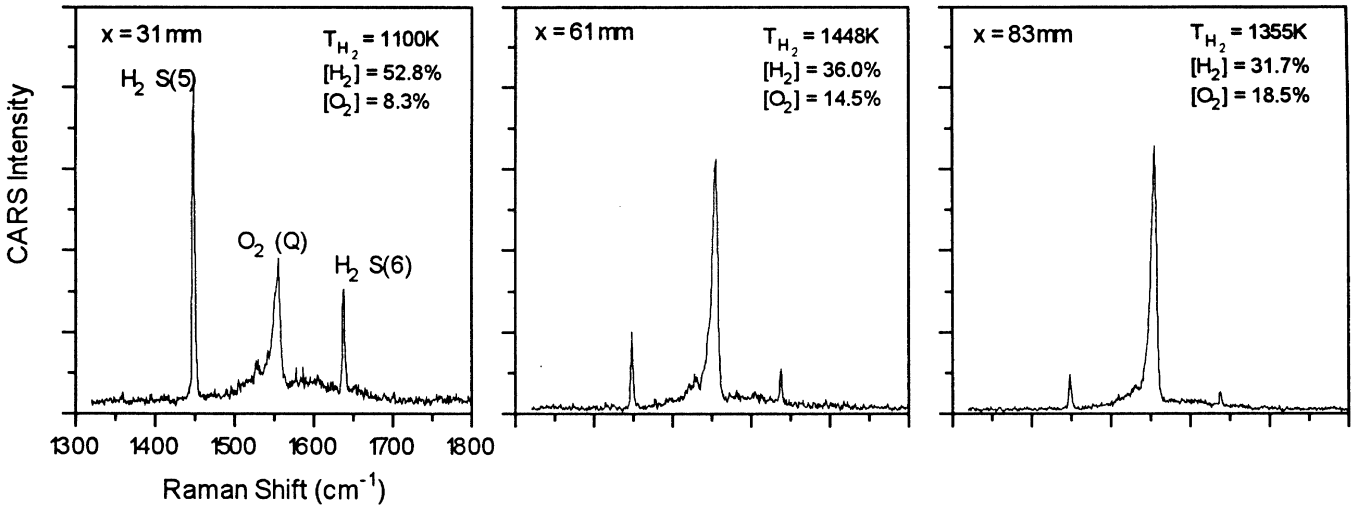

Fig. 12. H_2 and O_2 multiplex CARS spectra taken in the test sections of the H_2-air supersonic combustor. The measured temperatures and the mole fractions of H_2 and O_2 are denoted in the figures. T_{H_2} is the temperature derived from the intensity ratios of the H_2 S(5) and S(6) lines, [H_2] the mole fraction of H_2 derived from the H_2 S(6) line, and [O_2] the mole fraction of O_2 derived from the O_2 Q-branch CARS spectrum

laser shots (1 s), whereas the steady supersonic condition lasts for 3 s.

Three axial positions downstream of the H_2 injector are measured. The local temperature, T_{H_2}, is derived from the intensity ratio of H_2 S(5) and S(6). Moreover, the mole fraction of H_2, [H_2], is derived from the H_2 S(6) line, and the mole fraction of O_2, [O_2], is derived from the O_2 Q-branch spectrum. Results indicate that within a short distance away from the introduction of fuel, substantial mixing is achieved due to the use of the double-row injector with different angles. In addition, the mole fraction of H_2 decreases with increasing distance from the injector, while the O_2 mole fraction increases.

Efforts required to further improve the present methodology are the following. First, the nonresonant signal is an important factor for the accurate determination of species concentrations. However, the nonresonant susceptibility of a gas mixture is the mole fraction weighted average of the nonresonant susceptibilities of the individual molecular constituents and hence varies with the composition change at different combustion stages. Taking H_2/air premixed flame as an example, the major species involved are H_2, O_2, N_2, and H_2O. While the nonresonant susceptibilities of diatomic molecules are almost the same ($\approx 8.5 \times 10^{-18}$ (cm^3/erg)/amagat), the nonresonant susceptibility of water is about two times that of N_2($\approx 18.5 \times 10^{-18}$ (cm^3/erg)/amagat) [16]. Therefore, the mole fraction of water plays an important role for the calculation of the spectrally integrated nonresonant signal. If the mole fraction of water cannot be measured simultaneously, as a first cut its value could be estimated based on the local equilibrium assumption with a given measured temperature.

Second, detailed calibration experiments should be extended to a much wider range of temperature and concentrations of H_2 and O_2 by either nitrogen dilution or oxygen enrichment to the regular H_2/air mixtures.

Finally, the applicable range for the determination of the species mole fractions has to be improved, especially the lower detection limit. A possible improvement is to measure the resonant and nonresonant signals in situ. Furthermore, application of polarization-based techniques would also substantially increase the signal to noise ratio.

5 Concluding remarks

In the present study, a multiplex CARS is proposed for the simultaneous measurement of temperature and the mole fractions of H_2 and O_2. In particular, the O_2 Q-branched bandhead is sandwiched by the H_2 pure rotational lines of S(5) and S(6) when the temperature is beyond 700 K, which renders the simultaneous acquirement of the local temperature and species mole fractions with a single measurement.

Systematic calibration experiments are first carried out using a well-characterized flat-flame configuration, over a wide range of equivalence ratio for H_2/air premixed flames. Numerical calculations of the theoretical spectra are also performed for further correlations. In terms of the temperature calibration, the temperature data extracted by the intensity ratio of H_2 S(5) and S(6) are compared with those determined from the N_2 CARS spectra. The discrepancy is found to be around 4%.

Regarding the species calibration, the ratio of the spectrally integrated resonant and nonresonant signals has been applied to the obtained species mole fraction. Especially, the Q-branch of O_2 CARS spectrum and the S(6) line of H_2 CARS are utilized to determine the mole fractions of O_2 and H_2, respectively. The associated errors are found to be about 14% and 12%. Furthermore, the applicable range of the O_2 mole fraction is $\approx$ 4%–25%, while the lower detection limit of the H_2 mole fraction is around 10%.

Application of the present multiplex CARS to hydrogen-fueled supersonic combustion has been subsequently explored. Results demonstrate that such a multiplex CARS is a promising tool for the quantification of temperature distribution and mixing field within the supersonic combustor. A systematic investigation is currently under way, aiming to enhance the fundamental understanding of supersonic mixing and the associated combustion characteristics.

Acknowledgements. The Institute of Mechanics would like to acknowledge the support of the Expert Committee of Aerospace Technology Area of National 863 Program of China through Contract 863-2-2-3-3.

The participation of C.-J. Sung was supported by the Air Force Office of Scientific Research (AFOSR) under the technical monitoring of Dr. J.M. Tishkoff. The authors thank Professor C.K. Law of Princeton Uni-

versity for his discussions and for his encouragement of the collaboration. We also thank Mr. D.L. Zhu of Princeton University for the design and construction of the flat-flame burner.

References

1. A.C. Eckbreth, T.J. Anderson, B.M. Dobbs: Appl. Phys. B **45**, 215 (1988)
2. T.J. Anderson, A.C. Eckbreth: AIAA-90-0158 (1990)
3. M.W. Smith, Jr.O. Jarrett, R.R. Antcliff, G.B. Northam, A.D. Cutler, D.J. Taylor: J. Propul. Power **9**, 163 (1993)
4. J.R. Zhao, S.R. Yang, J.G. Li, G. Yu, C.J. Li: AIAA-97-0122 (1997)
5. A.C. Eckbreth: *Laser Diagnostics for Combustion Temperature and Species* (Abacus Press, Tunbridge Wells, Kent & Cambridge, Mass. 1988) pp. 220–300
6. J.P. Singh, F.Y. Yueh: Appl. Opt. **30**, 1967 (1991)
7. J.G. Li, G. Yu, Y. Zhang, Y. Li, D.X. Qian: J. Propul. Power **13**, 538 (1997)
8. G. Yu, J.G. Li, J.R. Zhao, S.R. Yang, C.J. Li: AIAA-96-4512 (1996)
9. R.E. Palmer: Sandia Report SAND89-8206 (1989)
10. R.J. Kee, J.F. Grcar, M.D. Smooke, J.A. Miller: Sandia Report SAND85-8240 (1985)
11. C.K. Law, C.J. Sung, G. Yu, R.L. Axelbaum: Combust. Flame **98**, 139 (1994)
12. R.J. Kee, A.E. Lutz, F.M. Rupley: *A Fortran Program for Calculating Chemical Equilibrium Using a Modified Solution Procedure of STANJAN* (1992)
13. T.J. Kim, R.A. Yetter, F.L. Dryer: Twenty-Fifth Symposium (International) on Combustion, The Combustion Institute, 759 (1994)
14. R.L. Farrow, R.E. Palmer: Opt. Lett. **12**, 984 (1987)
15. W.B. Roh, P.W. Schreiber, J.P.E. Taran: Appl. Phys. Lett. **129**, 174 (1976)
16. R.L. Farrow, R.P. Lucht, L.A. Rahn: J. Opt. Soc. Am. B **14**, 1241 (1987)